Plant Physiology
AMERICAN SOCIETY OF PLANT BIOLOGISTS

Plant Physiol. 2018 Feb; 176(2): 1751–1763. PMCID: PMC5813535
Published online 2017 Dec 14. doi: 10.1104/pp.17.01516 PMID: 29242376

Mineral Deposits in *Ficus* Leaves: Morphologies and Locations in Relation to Function[1]

Maria Pierantoni,[a] Ron Tenne,[b] Batel Rephael,[b] Vlad Brumfeld,[c] Adam van Casteren,[d] Kornelius Kupczik,[d] Dan Oron,[b] Lia Addadi,[a] and Steve Weiner[a,2]

[a]Department of Structural Biology, Weizmann Institute of Science, Rehovot 76100, Israel
[b]Department of Physics and Complex Systems, Weizmann Institute of Science, Rehovot 76100, Israel
[c]Department of Chemical Research Support, Weizmann Institute of Science, Rehovot 76100, Israel
[d]Max Planck Weizmann Center for Integrative Archaeology and Anthropology, Max Planck Institute for Evolutionary Anthropology, D-04103 Leipzig, Germany
www.plantphysiol.org/cgi/doi/10.1104/pp.17.01516
[2]Address correspondence to steve.weiner@weizmann.ac.il.
The author responsible for distribution of materials integral to the findings presented in this article in accordance with the policy described in the Instructions for Authors (www.plantphysiol.org) is: Steve Weiner (steve.weiner@weizmann.ac.il).
M.P. performed most of the experiments and analyzed the data; R.T. and B.R. helped perform some of the experiments and analyzed the data; V.B. provided expertise in microCT; A.v.C. and K.K. provided some of the materials; D.O. provided expertise in the optics and, together with L.A. and S.W., conceived the original project and supervised the experiments; M.P. wrote the original drafts; all authors participated in the writing.

Received 2017 Oct 19; Accepted 2017 Dec 9.

ABSTRACT

Ficus trees are adapted to diverse environments and have some of the highest rates of photosynthesis among trees. *Ficus* leaves can deposit one or more of the three major mineral types found in leaves: amorphous calcium carbonate cystoliths, calcium oxalates, and silica phytoliths. In order to better understand the functions of these minerals and the control that the leaf exerts over mineral deposition, we investigated leaves from 10 *Ficus* species from vastly different environments (Rehovot, Israel; Bologna, Italy; Issa Valley, Tanzania; and Ngogo, Uganda). We identified the mineral locations in the soft tissues, the relative distributions of the minerals, and mineral volume contents using microcomputed tomography. Each *Ficus* species is characterized by a unique 3D mineral distribution that is preserved in different environments. The mineral distribution patterns are generally different on the adaxial and abaxial sides of the leaf. All species examined have abundant calcium oxalate deposits around the veins. We used micromodulated fluorimetry to examine the effect of cystoliths on photosynthetic efficiency in two species having cystoliths abaxially and adaxially (*Ficus microcarpa*) or only abaxially (*Ficus carica*). In *F. microcarpa*, both adaxial and abaxial cystoliths efficiently contributed to light redistribution inside the leaf and, hence, increased photosynthetic efficiency, whereas in *F. carica*, the abaxial cystoliths did not increase photosynthetic efficiency.

Mineral deposits are an integral part of many plant leaves, but not all leaves contain mineral deposits. In the leaves that do have minerals, the mineral type, morphology, and distributions within the leaves are under strict control (Arnott and Pautard, 1970; Webb, 1999). In fact, mineralization in certain leaves is a well-preserved trait throughout evolution, indicating that such controlled mineralization is

advantageous (Kausch and Horner, 1982; Trembath-Reichert et al., 2015). The most widespread leaf minerals are silica and calcium oxalate and, to a lesser extent, amorphous calcium carbonate (ACC; Arnott, 1982). In general, calcium oxalate crystals occur in different anatomical locations, most commonly in the palisade or along the veins (Horner et al., 1978; Franceschi and Horner, 1980; Webb and Arnott, 1981; Arnott, 1982; Webb, 1999). Many roles have been ascribed to calcium oxalates in leaves, including calcium regulation, detoxification of heavy metals, leaf defense, and an internal CO_2 source (Finley, 1999; Franceschi and Nakata, 2005; Tooulakou et al., 2016). Silica deposition (phytoliths and small particles) can occur in any part of the leaf epidermis, leaf mesophyll, and the vascular tissue (Perry and Fraser, 1991; Currie and Perry, 2007; Law and Exley, 2011; Horner et al., 2015; Strömberg et al., 2016). Phytoliths are thought to reduce radiation damage and to play a role in many other physiological processes, such as the regulation of other nutrients, pathogen resistance, enhancing mechanical properties, and defense (McNaughton et al., 1985; Marschner et al., 1990; Cai et al., 2009; Gautam et al., 2016). Cystoliths are calcified bodies deposited in specialized epidermal cells (Meyen, 1839; Ajello, 1941; Omori and Watabe, 1980; Setoguchi et al., 1989). Cystoliths are composed of hydrated ACC (Ajello, 1941).

In many cases, the cystolith is connected to the outer cell wall through an internal silica stalk that helps to stabilize the ACC phase (Setoguchi et al., 1989; Sugimura et al., 1999; Gal et al., 2010, 2012b). It has been demonstrated that, in the palisade mesophylls of *Ficus microcarpa*, *Morus alba*, *Abelmoschus esculentus* (okra), and *Peperomia obtusifolia*, cystoliths or calcium oxalates function as light scatterers, increasing the leaf photosynthetic yield (Kuo-Huang et al., 2007; Detmann et al., 2012; Gal et al., 2012a; Horner, 2012; Horner et al., 2012; Pierantoni et al., 2017). Furthermore, in okra, the locations of calcium oxalate and silica deposits are not independent. The two minerals can form a complex system with a highly regulated relative distribution (Pierantoni et al., 2017). Here, we study 10 species within the vast *Ficus* genus (about 850 species; Janzen, 1979), as these leaves contain all three of the major mineral types found in leaves (Arnott and Pautard, 1970; Webb, 1999). The *Ficus* genus is physiologically adapted to diverse environments, and *Ficus* species can inhabit extremely different climatic regions in the form of trees, shrubs, stranglers, and vines (Herre et al., 2008). *Ficus* species are distributed throughout rainforests, canopies, savannahs, river sides, xeric environments, and cliffs (Corner, 1952; Janzen, 1979; Harrison, 2005) and, consequently, are a good model in which to study the effects of different environments and climates on species belonging to the same genus. *Ficus* trees also have some of the highest rates of photosynthesis (Patiño et al., 1994; Zotz et al., 1995; Herre et al., 2008) and, therefore, are a good system in which to study the possible functions of minerals in light manipulation. However, there is no comprehensive record of the mineral presence and distribution in the different *Ficus* species. Furthermore, no information on the possible mineral functions in relation to light is available. In an effort to better understand the functions of leaf minerals, we investigate here the mineral locations in the soft tissues, the relative locations of the minerals, the mineral volume contents, and the relations of the mineral volumes to the leaf environmental conditions. We analyzed 10 *Ficus* species (two of which are from different locations, giving a total of 12 different specimens) from vastly different environments. The aims of this comparative study are to document the 3D distributions of the minerals and, by so doing, obtain a better understanding of the functions of different minerals in leaves. We focus on *Ficus* species in order to establish the generality of the observations in one genus, particularly in relation to light exploitation.

RESULTS

3D Maps of Minerals and Soft Tissues in *Ficus* Leaves

Detailed 3D maps of the spatial locations of the minerals in leaves from 10 *Ficus* species were obtained by microcomputed tomography (microCT). To establish whether there is any correlation between the environment in which the plants grow and minerals in the leaves, we examined leaves of plants from Rehovot, Israel (*Ficus binnendijkij*, *Ficus elastica*, *Ficus microcarpa*, *Ficus carica*, and *Ficus religiosa*), from the Ngogo National Park in the Uganda tropical rainforest (Lwanga et al., 2000; Watts et al., 2012; *Ficus varifolia*, *Ficus mucoso*, and *Ficus exasperata*), from the Issa Valley in the Tanzanian savannah woodland (Stewart and Piel, 2014; Piel et al., 2015; *Ficus lutea*, *F. varifolia*, and *Ficus sp*), and from Bologna, Italy (*F. carica*). Leaves from the same species, *F. carica* and *F. varifolia*,

were taken from trees grown in different environments and compared. Leaves of *F. varifolia* were taken from trees growing in the Tanzanian savannah woodland and compared with those from the Ugandan tropical rainforest, and leaves of *F. carica* from Rehovot, Israel, were compared with those from Bologna, Italy.

The microCT 3D cross-sectional perspective views (Fig. 1, A–L) show that all 10 *Ficus* species have minerals, and these minerals are deposited in the epidermis and in the mesophyll. MicroCT scans of different leaves from different trees in the same location (*F. carica*, *F. elastica*, and *F. microcarpa*) showed the same mineral distributions for leaves belonging to the same tree species, and scans taken through the whole leaf thickness and in different areas of the same leaf showed that mineral distributions are almost identical. Consequently, the 1-mm^3 tissue sections examined here are good representatives of the mineral distribution in the entire leaf. The mineral distributions are clearly asymmetric when comparing the upper abaxial part with the lower adaxial part of the leaf. The only exception is *F. religiosa*, which does not deposit minerals in the epidermis but only in the mesophyll (Fig. 1L). The only anatomical location where mineral deposits (calcium oxalate druses and prisms) are present in all 10 species is the central vein (Table I). The other mineralized deposits, hairs (trichomes) composed of silica and ACC cystoliths, are present in specific anatomical locations depending on the species (Table I). Note that there are no significant differences between leaves belonging to the same species but from different environments (*F. varifolia*, Fig. 1, E and G; *F. carica*, Fig. 1 F and H).

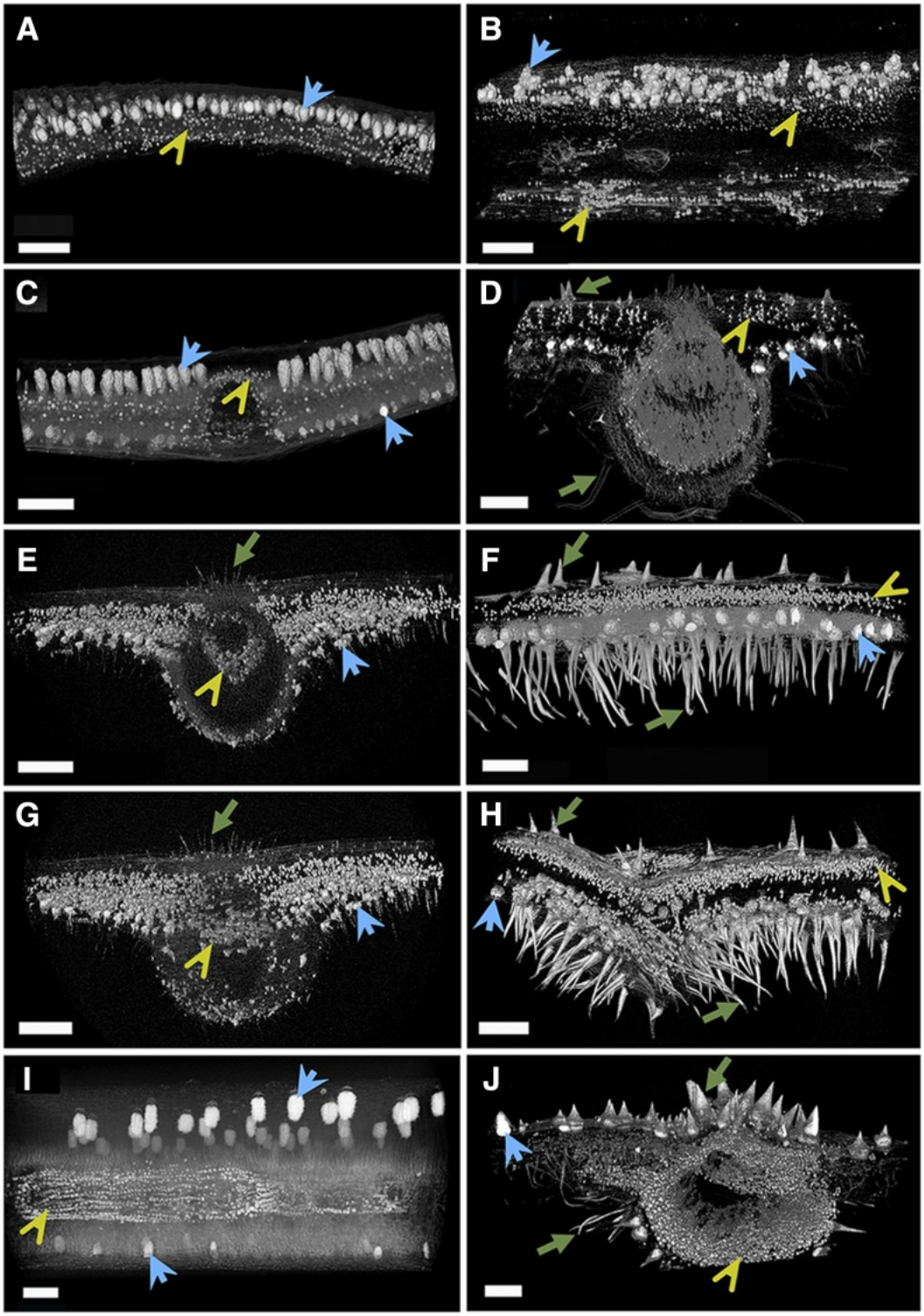

Open in a separate window

Figure 1.

MicroCT 3D cross-sectional perspective views of minerals (highly contrasting bodies) and soft tissues in *Ficus* leaves. The leaf orientation was chosen to better visualize mineral distribution (major vein cross section or minor vein longitudinal view). All leaves are shown with their upper adaxial surfaces on the top. A, *F. binnendijkij* (Israel), longitudinal view. B, *F. lutea* (Tanzania), longitudinal view. C, *F. elastica* (Israel), longitudinal view. D, *F. microcarpa* (Israel), cross section. E, *F. varifolia* (Uganda), cross section. F, *F. carica* (Israel), longitudinal view. G, *F. varifolia* (Tanzania), cross section. H, *F. carica* (Italy), longitudinal view. I, *F. mucoso* (Uganda), cross section. J, *F. sp* (Tanzania), cross section. K, *F. exasperata* (Uganda), cross section. L, *F. religiosa* (Israel), cross section. M, General schematic representation of the

most common types and locations of minerals deposited in the leaves of *Ficus* leaves examined. In all images, green arrows indicate silica deposits, light blue short arrows indicate cystoliths, and yellow arrowheads indicate calcium oxalates. Bars = 200 µm.

Table I.

Distributions and sizes of cystoliths, phytoliths, trichomes, and calcium oxalates on the upper adaxial side, the lower abaxial side, and around the veins of the 10 *Ficus* species (for two of the species, data are presented for leaves obtained from two different environments)

Species	Approximate leaf thickness (µm)	Adaxial side			Abaxial side			Veins	
		Cystoliths (µm)	Phytoliths (µm)	Trichomes (µm)	Cystoliths (µm)	Phytoliths (µm)	Trichomes (µm)	Calcium oxalates on the outer surface (µm)	Calcium oxalates on the inner surface (µm)
F. Binnendijkii (Israel, Mediterranean semi-arid region)	250	80±10	_	_	_	_	_	15±3	_
F. lutea (Tanzania, savannah woodland)	500	60±5	_	_	_	_	_	5±2; 20±4	_
F. elastica (Israel, Mediterranean semi-arid region)	1000	140±20	_	_	60±10	_	_	15±2; 25±3	_
F. microcarpa (Israel, Mediterranean semi-arid region)	300	100±10	_	_	40±10	_	_	5±2; 15±5	_
F. religiosa (Israel, Mediterranean semi-arid region)	200	_	_	_	_	_	_	10±2; 40±5	10±2; 40±5
F. varifolia (Tanzania, savannah woodland)	200	_	_	80±40 (above the veins)	30±5	_	60±30	10±3	10±4; 25±5
F. varifolia (Uganda, tropical rainforest)	200	_	_	80±40 (above the veins)	30±5	_	60±30	10±4	10±5; 25±7
F. carica (Israel, Mediterranean semi-arid region)	300	-	170±100	80±30	100±30	_	350±150	10±3	_
F. carica (Italy, Mediterranean region)	300	-	300±200	80±30	100±30	_	350±150	10±3	_
F. Mucoso (Uganda, tropical rainforest)	300	_	200±100	60±30	45±5	_	500±200	5±1	5±2; 15±2
F. sp (Tanzania, savannah woodland)	300	20±5	_	300±100	80±30	_	300±100	5±2; 25±3	_
F. exasperata (Uganda, tropical rainforest)	200	50±15; 200±20	_	_	50±15; 200±2 (under the veins)	_	300±250	5±3; 15±4	5±3; 25±5

When two populations of different sizes are present, averages and standard deviations for both are shown. Note that the leaf cross-section thickness does not include the thickness of the central vein, which can protrude by hundreds of micrometers (Fig. 1). The domestic Ficus types are in white rows, and the wild types are in green rows.

The anatomical locations of all the mineral deposits in these 10 leaves are shown schematically in Figure 1M. A few generalizations can be made about the mineral distributions. To the best of our knowledge, minerals are present in all *Ficus* species. Vein-associated calcium oxalate deposits are present in all 10 species examined here, but their specific distributions around the vein vary among the leaves. Cystoliths can be deposited in the upper and lower epidermis extending, in some cases, into the mesophyll. In the upper epidermis, cystoliths have an elongated morphology, whereas the cystoliths on the lower side of the leaf are more spherical. In all the cases studied, cystolith deposition occurs preferentially on one side of the leaf, either adaxially (upper surface) or abaxially (lower surface; Fig. 1M). In the leaves of *F. microcarpa* and *F. elastica*, cystoliths appear preferentially on the adaxial side, but smaller cystoliths also are deposited in the abaxial lower epidermis (Supplemental Fig. S1, A and B). In *Ficus sp*, where the main cystoliths are abaxial, irregular small cystoliths are distributed

unevenly in the adaxial upper epidermis (Supplemental Fig. S2C). Note that no cystoliths are deposited by *F. religiosa* (Fig. 1L). This indicates that cystoliths augment a function in *Ficus* leaves but do not perform an essential function.

Silica forms in three different anatomical locations: cell walls, the trichomes, and stalks within and protruding from the cystoliths. Note that only relatively large deposits of silica can be identified by microCT (Pierantoni et al., 2017). There might be a lot more silica in these leaves in the form of small finely dispersed deposits, as was revealed by staining in the case of the okra leaves (Pierantoni et al., 2017). Silica deposition in the upper epidermis is well developed in leaves in which most of the cystoliths are on the lower side.

Only a few of the species examined have well-developed silicified trichomes, and these are located on both surfaces. Silicified trichomes never form above cystoliths. Leaves of *F. exasperata* from Uganda (Fig. 1K) have a unique mineral deposit, namely mineralized spikes composed of ACC and silica.

Elongated Cystoliths in the Upper Epidermis

Elongated ACC cystoliths (Fig. 2) are formed in the upper epidermis and extend into the palisade mesophyll (Fig. 1, A–D). The long axes of these cystoliths can vary from around 60 µm in *F. lutea* (Fig. 2B) to around 140 µm in *F. elastica* (Fig. 2C). All the elongated cystoliths contain a central silica stalk that is either completely inside the cystolith (*F. microcarpa* in Fig. 2D) or extends out of the cystolith. This extension can be in the form of a rod (*F. lutea* in Fig. 2B), a silica dome above the cystolith (*F. binnendijkij* in Fig. 2A), or a radial structure (*F. elastica* in Fig. 2C). When the leaf is viewed in planar projection, the cystoliths are never located above the veins and, consequently, the mineral distributions of cystoliths and calcium oxalates never overlap (Supplemental Fig. S2, A and B). In the epidermis of the leaves forming elongated cystoliths, no silica deposits are visible (Fig. 1, A–D).

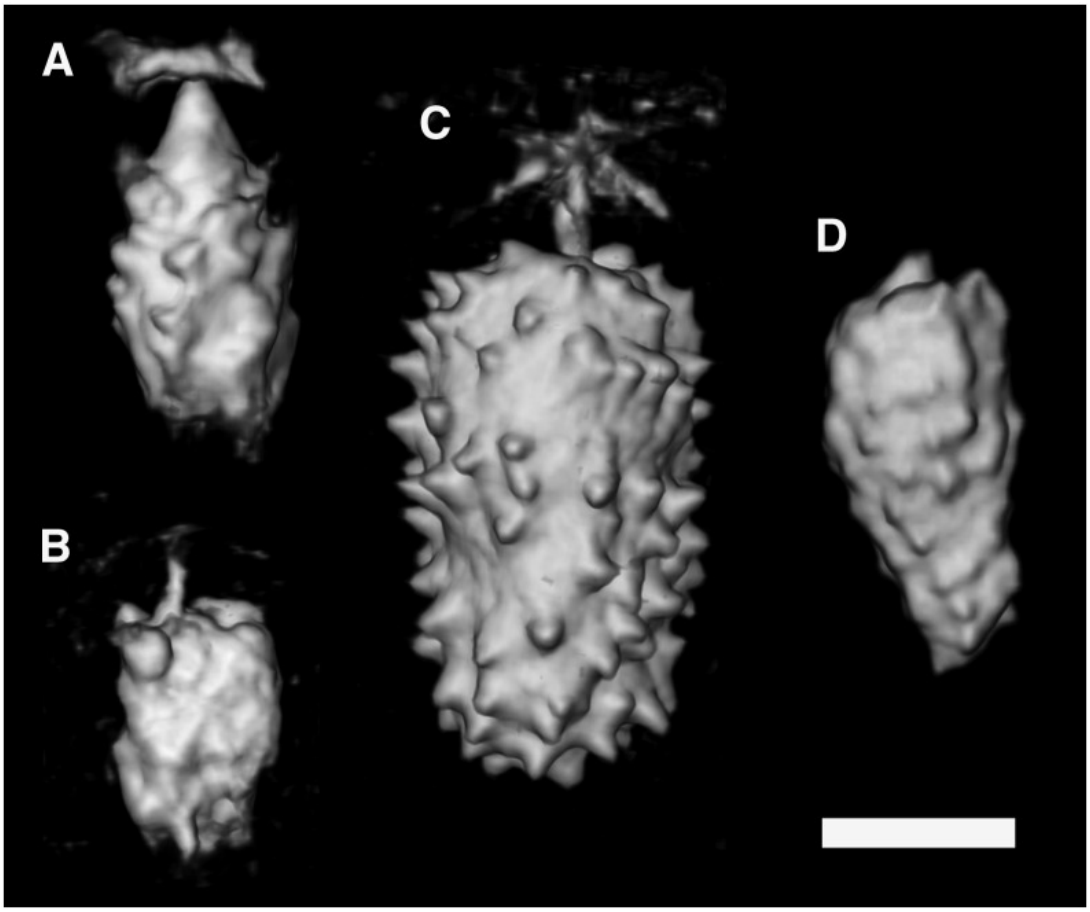

Figure 2.

MicroCT images of elongated cystoliths deposited in the upper epidermis. A, *F. binnendijkij*. B, *F. lutea*. C, *F. elastica*. D, *F. microcarpa*. Bar = 50 µm.

Spherical Cystoliths in the Lower Epidermis

In some leaves, spherical ACC cystoliths (Fig. 3) are formed in the lower epidermis and extend into the spongy mesophyll (Fig. 1, E–K). The diameters of these cystoliths can vary significantly depending on the species, from around 30 µm in *F. varifolia* (Fig. 3A) to around 70 µm in *Ficus sp* (Fig. 3D). Contrary to what is observed for the upper epidermal cystoliths, the lower epidermal cystoliths are densely packed, and in some cases, calcium oxalates and cystoliths can overlap in planar projection and be almost in contact (Supplemental Fig. S2, C and D). An elongated cylindrical stalk of silica is seen inside all the lower epidermal cystoliths and protrudes from them (Fig. 3, A, B, and D), except for *F. mucoso*, where the stalk is completely inside the cystolith (Fig. 3C).

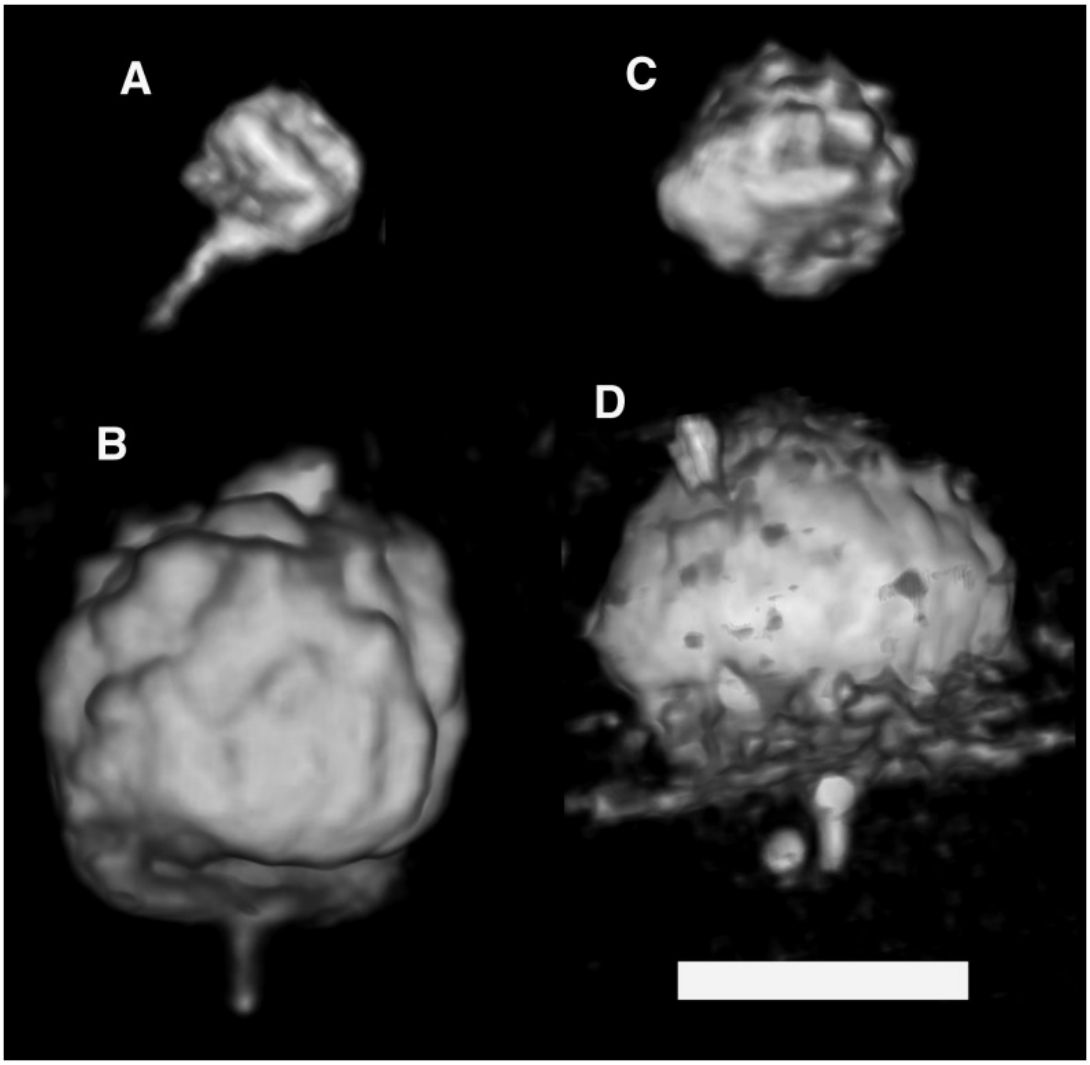

Figure 3.

MicroCT images of cystoliths deposited in the *Ficus* lower epidermis. A, *F. varifolia*. B, *F. carica*. C, *F. mucoso*. D, *F. sp*. Bar = 50 µm.

Calcium Oxalate Crystals long the Veins

In all the studied mature leaves, calcium oxalate crystals are deposited along the veins in lines parallel to the vein major axes. In order to understand the exact locations of the minerals around the vein and to acquire information about the vein structure, a method is required to increase soft tissue contrast without any staining and without inducing extensive drying. Our approach was to use phase-contrast enhancement in the microCT to visualize the soft tissue structure (for details, see “Materials and Methods”).

Calcium oxalates are deposited in the phloem in vascular parenchyma (Fig. 4, A′ and C′), along the vein bundles (Fig. 4, B, D, and F), or in the ground tissue that provides support to the vein (Fig. 4E′). The vein bundle distribution seems to determine the deposition pattern for the calcium oxalates, namely in parallel lines. The deposition of calcium oxalates in the phloem and in the ground tissue was already observed in other *Ficus* species (Araújo et al., 2014; Chantarasuwan et al., 2014).

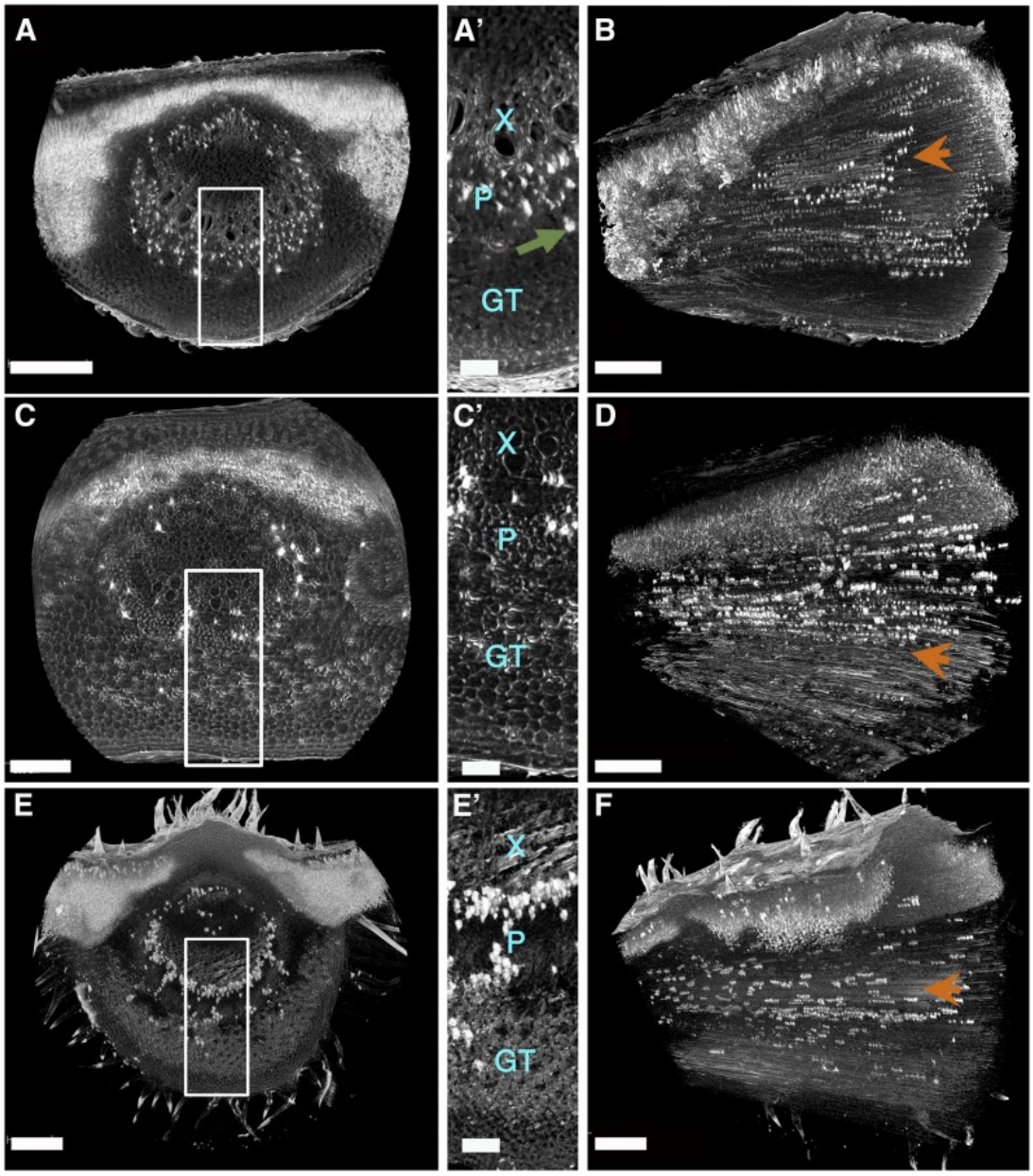

Figure 4.

MicroCT images of calcium oxalate crystals deposited in *Ficus* main veins. A and B, *F. microcarpa*. C and D, *F. elastica*. E and F, *F. carica*. The first column shows cross-sectional perspective views perpendicular to the vein direction, the second column shows higher magnification views of the area highlighted in the rectangle, and the third column shows side views of the vein. The arrowheads indicate the direction of the vein bundles. GT, Ground tissue; P, phloem; X, xylem. The green arrow points to a druse. Bars = 200 μm (A–F) and 50 μm (A′, C′, and E′).

Here, we present three representative cases. In *F. microcarpa* (Fig. 4, A and B), two different types of calcium oxalates can be observed. Druses are deposited along the bundles in the ground tissue (mostly adaxially), whereas smaller single prismatic crystals and smaller druses are deposited in the phloem (mostly abaxially). In *F. elastica*, both druses and prismatic crystals are deposited, mostly in the phloem and some in the ground tissue, mostly abaxially (Fig. 4, C and D). In *F. carica*, simultaneous druse and prismatic crystal deposition starts several days after the leaf is formed and continues until the leaf reaches its final size (Supplemental Fig. S3). The calcium oxalates are deposited mostly in the phloem, with few minerals extending into the ground tissue (Fig. 4, E and F). A cross section of *F. microcarpa* phloem shows that druses and prisms are deposited intracellularly (Supplemental Fig. S4).

Silicified Trichomes and Phytoliths in the Upper and Lower Epidermis

In all the *Ficus* leaves forming cystoliths in the lower epidermis, silica is deposited in the trichomes and in cell walls (Fig. 5). Trichomes can vary in shape and size. In the upper epidermis of *F. carica* and *F. mucoso*, the trichomes have conical morphologies (Fig. 5, A and D) and the epidermal cell walls have silica deposits (Fig. 5, C and E). In the lower epidermis of all the silica-depositing species, the trichomes have an elongated and thin cylindrical structure. Even though, in the lower epidermis, silica trichomes can be very densely packed, there are no silica deposits associated with cystoliths (Fig. 5, B and F).

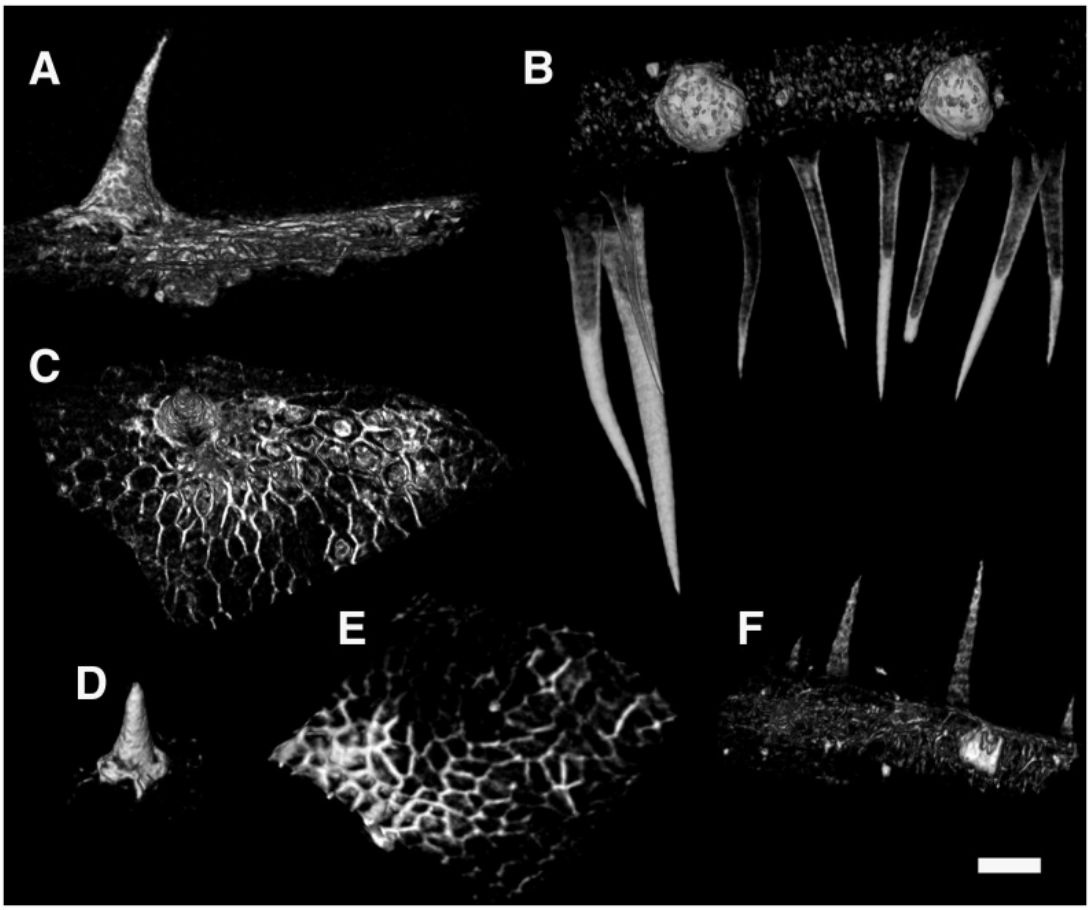

Figure 5.

MicroCT images of silicified trichomes and phytoliths. A, Side view of a trichome and silica deposits in the upper epidermal cell walls of *F. carica*. B, Silicified lower epidermal trichomes and cystoliths in *F. carica*. C, Top view of A. D, An upper epidermal trichome in *F. mucoso*. E, Silica deposits in the upper epidermis cell walls of *F. mucoso*. F, Silicified upper epidermal trichomes in *F. sp.* Trichomes and the small cystoliths deposited in the upper epidermis never overlap. Bar = 50 µm.

Silica-Cystolith Trichome Spikes

F. exasperata leaves have unique mineralized cone-shaped trichomes, which we refer to as spikes. These spikes are located in the upper epidermis and all around the veins (Fig. 1K). The spikes (50–200 µm long) consist of an ACC core inserted in a shell of silica (Fig. 6, A and B). The two minerals are separated by a cavity, and there are no visible silica deposits inside the ACC (Fig. 6, A′ and B′). These mineralized units seem to be a unique variant of the conic silicified trichomes observed in *F. carica* and *F. mucoso* (Fig. 5, A and D), but in *F. exasperata*, the spikes are associated with ACC deposits. The deposits grow outward from the epidermis and do not extend into the mesophyll, as do the cystoliths (

Fig. 1K). These leaves are the only case studied here where ACC deposits in the upper epidermis are above the veins. Only a few micrometers separate the spikes from the calcium oxalate deposits that surround the veins.

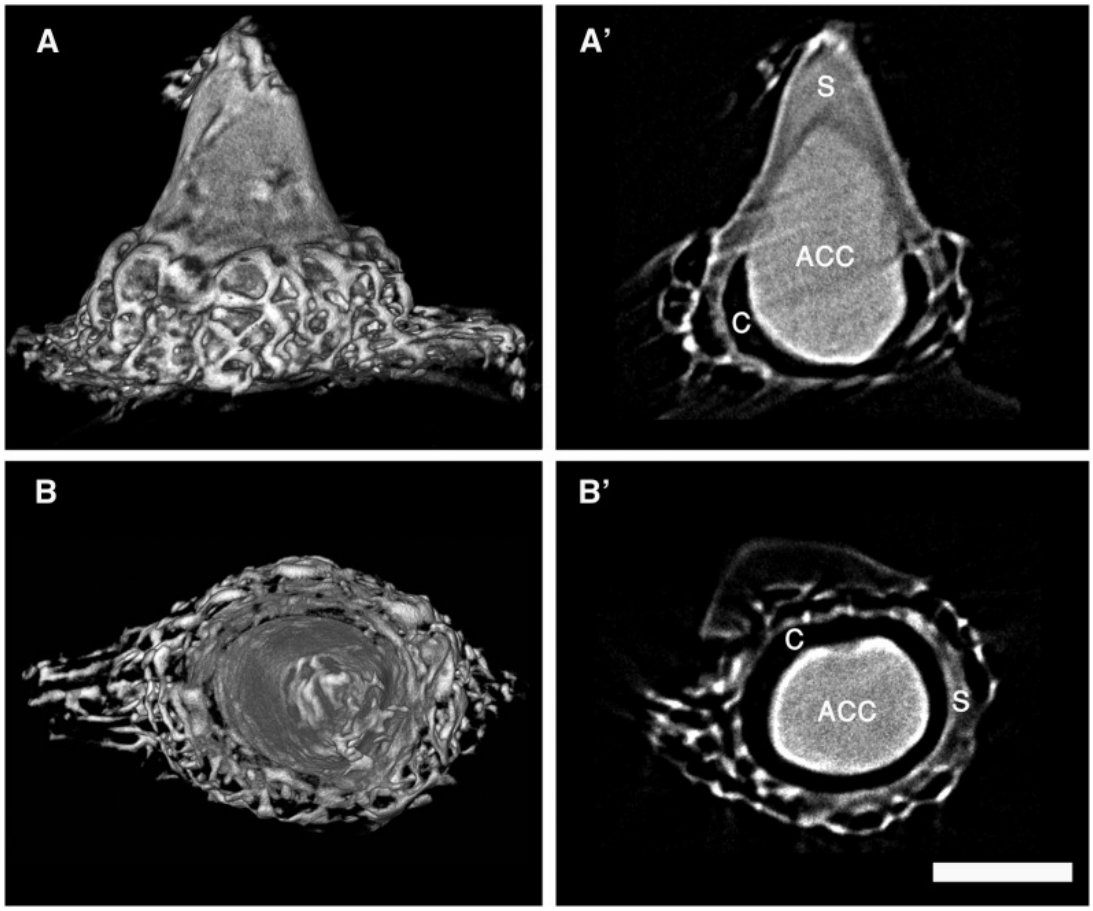

Figure 6.

MicroCT images of the spikes in *F. exasperata* leaves. A, Side view of one mineralized spike after extraction. A′, Cross section through A showing the external silica shell (S), the internal ACC, and the cavity (C) between the two minerals. No silica stalk is deposited in the ACC. B, Top view of the extracted spike. B′, Cross section of B showing the internal structure. Bar = 50 μm.

Mineral Volume Content in Relation to Environment and Plant Domestication

Ficus trees from different environments were studied in order to determine if mineral deposition could be affected by environmental factors (Table II). The volume percentage occupied by calcium minerals in the leaf varies greatly between the *Ficus* trees studied (Table II). The percentages range from 0.4% of the occupied volume in the case of *F. lutea* from the Tanzanian savannah woodland to the exceptionally high 3.2% of *F. exasperata* from the Ugandan tropical rainforest. The values, however, do not show any correlation between environment and mineral volume percentage. Within the same species from different environments, mineral content (calculated as volume percentage occupied by minerals), together with mineral morphologies and location, is highly preserved, as occurs for *F. carica* and *F. varifolia*.

Table II.

Mineral deposits in relation to the environment

Origin	Species	Volume percentage occupied by calcium minerals	Silica phytoliths
Ngogo, Uganda, (tropical rainforest)	*F. exasperata*	3.2%	Yes
	F. mucoso	0.6%	few
	F. varifolia	0.7 %	few
Issa valley, Tanzania (savannah woodland)	*F. varifolia*	0.8%	few
	F. sp	1.6%	yes
	F. Lutea	0.4%	no
Rehovot, Israel (Mediterranean semi-arid region)	*F. microcarpa*	1.3%	no
	F. elastica	1.4%	no
	F. religiosa	1.7%	no
	F. binnendijkii	1.7%	no
	F. carica	1.6%	yes
Bologna , Italy (Mediterranean region)	*F. carica*	1.5%	yes

The domestic types are in white rows, and the wild types are in green rows.

Based on this limited sample set, we can conclude that the survey did not show significant differences in mineral content and distribution either between leaves from young and old trees or between undergrowth plants, growing in the shade (*F. varifolia* from Tanzania; *F. sp*, *F. elastica*, and *F. religiosa*), and tall trees, which are exposed to direct light (*F. exasperata*, *F. mucoso*, and *F. varifolia* from Uganda; *F. lutea*, *F. microcarpa*, and *F. carica* from Israel; and *F. carica* from Italy). Temperature variations throughout the year and the daily availability of water throughout the year also do not seem to directly affect the mineral deposition process. Furthermore, both wild types and domestic types were studied, and the domestication seems not to have affected either the mineral content or the mineral location, which are uniformly distributed through all the species.

Some Cystoliths Increase the Photosynthetic Efficiency

Ficus species originated in areas with high light intensity (Kislev et al., 2006), and based on our observations, they seem to have preserved their mineralization densities and locations within the same species, independent of environmental influences. It was shown previously for *F. microcarpa* that adaxial cystoliths scatter light inside the tissue and, in this way, increase the total photosynthetic yield of the leaf (Gal et al., 2012a).

It was recently shown that leaves can adapt to optimize not only direct illumination reaching the adaxial side but also to tune the level of illumination from the abaxial side (Horner et al., 2017). We examine here the possibility that the leaves of some of the species in this study enhance photosynthesis by redistributing light through cystoliths from both the adaxial and abaxial surfaces. The light intensities reaching the upper and lower sides of *Ficus* leaves were measured with a diode-based power sensor. The measurements showed that around midday in Israel, in March, not only the leaf adaxial sides but also the abaxial sides undergo photoinhibition. Above 1,000 µmol (photon) m^{-2} s^{-1} was measured from the abaxial side of the leaf, due to the strong reflection coming from the ground (Supplemental Table S1). The specific value depends also on the leaf orientation and on the nature of the ground surface. This raises the possibility that redistribution of light impinging upon the leaf abaxial side into the deeper parts of the leaf could be beneficial in terms of photosynthetic efficiency.

We studied two different cases: *F. microcarpa* leaves, where cystoliths are present on both sides (Fig. 1D), and *F. carica* leaves, where cystoliths are present only on the abaxial side and abundant phytoliths are present (Fig. 1F). Micromodulated fluorimetry measures the chlorophyll fluorescence during laser illumination. Chlorophyll fluorescence is an escape pathway of absorbed light that is not used for chemical reactions. As such, the fluorescence measurement quantifies the unused portion of light and, therefore, serves as an inverse proxy for the efficiency of the light cycle within the photosynthetic apparatus (Papageorgiou, 2007). Under light illumination flux exceeding the photoinhibition threshold, reaction centers gradually close and the chlorophyll remains excited until it releases the energy either in the form of a photon or as heat (Powles, 1984).

Both minerals and areas without cystoliths (control areas) were excited by a focused laser beam (12 µm diameter) whose wavelength is within the chlorophyll absorption spectrum (635 nm). The minerals and control areas were located by transmittance of light through the leaf (Supplemental Fig. S5, A–G). Then, chlorophyll fluorescence was imaged onto a CCD camera (Supplemental Fig. S5, A′–G′). The total intensity of the collected fluorescence was integrated and shown as histograms (Fig. 7, A–D). Each bar of the histogram represents the number of recorded events for a given fluorescence intensity. The lower the intensity, the more efficient the photosynthetic process. Note that the volume occupied by the cystoliths (~50 × 50 × 100 µm) is less than 5% of the leaf volume from which the fluorescence is collected (160 × 160 × 300 µm; Supplemental Fig. S5), whereas the decrease in fluorescence intensity, when measured in *F. microcarpa*, is ~3- to 4-fold. Under these conditions, the effects due to local differences caused by the cystolith presence are negligible.

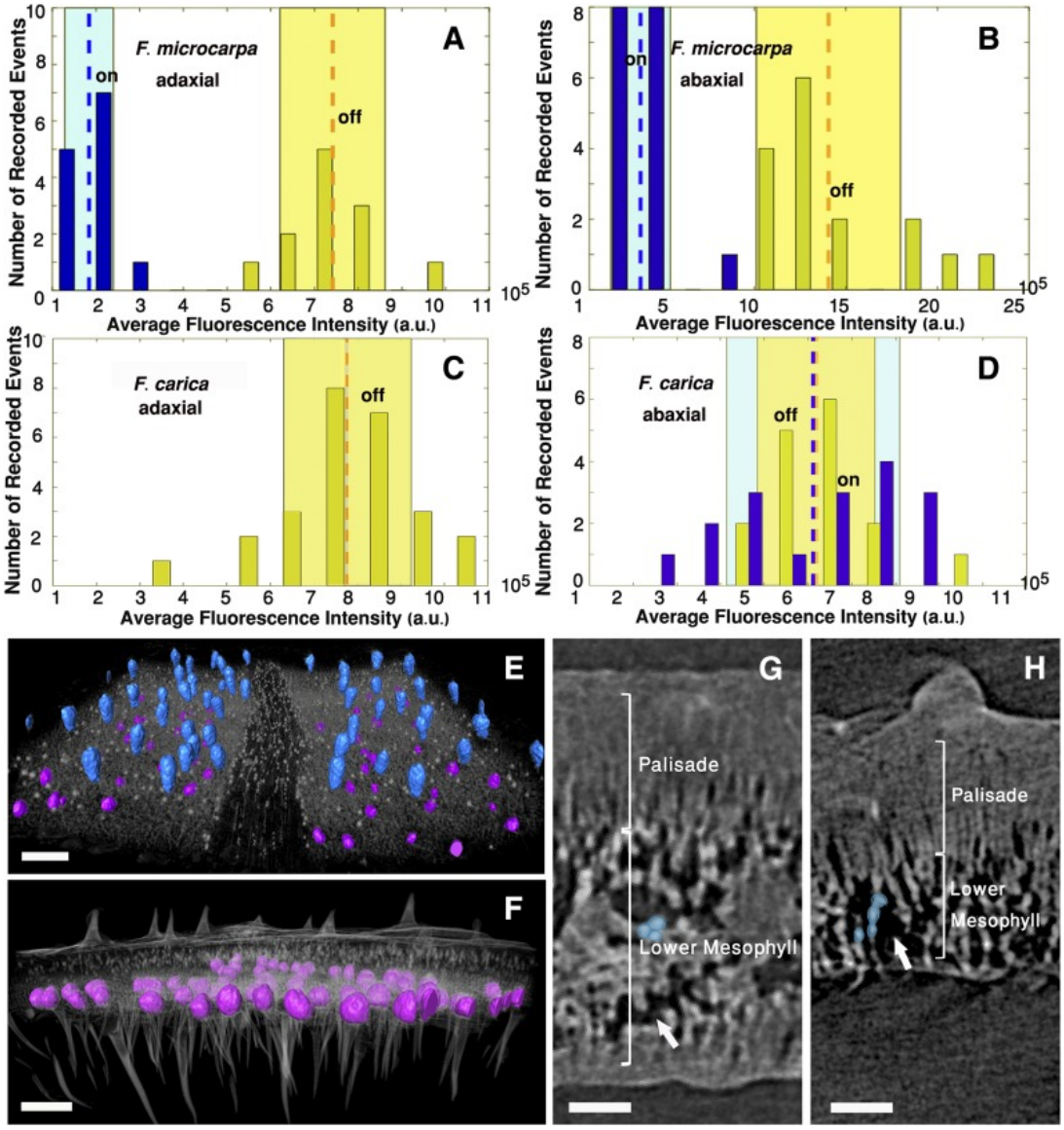

Figure 7.

A to D, Bar plots of the number of recorded events (*y* axis) having the indicated spatially integrated fluorescence intensity (*x* axis) from microfluorimetry curves, obtained when illuminating a cystolith (on; blue) versus those obtained when illuminating off-cystolith locations (off; yellow). The dashed line represents the mean intensity for each distribution; the shaded areas indicate SE. A, *F. microcarpa* adaxial side. B, *F. microcarpa* abaxial side. C, *F. carica* adaxial side. D, *F. carica* abaxial side. E and F, MicroCT volumes of an *F. microcarpa* leaf (E) and an *F. carica* leaf (F). Adaxial cystoliths are blue and abaxial cystoliths are purple. Bars = 200 µm. G and H, MicroCT ortho slices of an *F. microcarpa* leaf (G) and an *F. carica* leaf (H) showing the soft tissue structure. The lower mesophyll cells (representative cells marked in blue) are densely packed with few air spaces (arrow in G) in *F. microcarpa* and loosely packed with big air spaces (arrow in H) in *F. carica*. Bars = 50 µm.

In *F. microcarpa* on the adaxial side, the fluorescence intensity is weaker than on the abaxial side (Fig. 7, A and B, yellow bars). Since most of the light is absorbed within about one scattering length in the leaf tissue such that loss of back-scattered fluorescence in the leaf is relatively small, the measured fluorescence intensity serves as a good quantitative estimator of the emitted fluorescence from inside the leaf (Powles, 1984). The reduced fluorescence intensity when illuminating the adaxial side thus means that the amount of wasted light is lower when the light reaches the leaf adaxially, compared with the abaxial surface. When the laser light illuminates a cystolith, the wasted portion of light is reduced by 4.1 and 3.7 times, respectively, for adaxial cystoliths and adaxial cystoliths, relative to areas that do

not contain cystoliths (Fig. 7, A and B). This shows that the cystoliths on both surfaces are functioning to scatter light into light-deprived interior regions within the leaf and, thus, are enhancing photosynthesis. Note too that minerals on the upper and lower sides of the leaf do not overlap spatially when viewed in projection (Fig. 7E). Consequently, the interior areas illuminated by the scattered light from the adaxial and abaxial sides also do not overlap substantially. This distribution is beneficial for light-harvesting, since a more uniform illumination within the leaf leads to a reduced loss due to either fluorescence or, later, photoinhibition (Powles, 1984). *F. microcarpa* leaves have one layer of dense palisade on the adaxial side, one layer of dense mesophyll juxtaposed to the lower epidermis, and air spaces in the center between the two dense layers (Fig. 7G). The cells are so densely packed in the two layers that the presence of scatterers increases significantly the level of illumination in the tissue located in the leaf center.

In *F. carica*, the amount of wasted light emitted as fluorescence is comparable on the two leaf sides (Fig. 7, C and D, yellow bars). Furthermore, since the fluorescence intensity is comparable for measurements performed on cystoliths and off cystoliths, the cystoliths do not seem to have any effect (Fig. 7, C and D).

In *F. carica*, cystoliths protrude from the lower epidermis into the mesophyll and the distance between them is irregular (Fig. 7F). In contrast to *F. microcarpa*, only the adaxial side has a dense palisade layer, whereas the lower mesophyll is formed by small loose cells with air spaces that traverse the whole layer down to the leaf surface (Fig. 7H). Due to the cell organization in the lower mesophyll, the light can probably be efficiently transmitted deeper into the leaf without the need of cystoliths, possibly explaining why there is no difference in measurements taken on cystoliths and off cystoliths.

DISCUSSION

Leaf cross sections are strikingly asymmetric. On the adaxial side, the elongated and densely packed palisade cells are optimized for light harvesting. On the abaxial side, the loose spongy cells and the air spaces facilitate gas exchange (De Lucia et al., 1991; Fukushima and Hasebe, 2014). This raises the possibility that the different minerals and their distributions reflect these major functions. The adaxial/abaxial asymmetry is well reflected in the mineral distributions of all the *Ficus* species examined, with the exception of *F. religiosa*, which has mineral only around the veins. The central veins, besides fulfilling physiological functions, contribute significantly to the mechanical properties of the leaf (Lucas et al., 1991; Choong, 1996). In all the leaves studied, the veins are always associated with minerals. We note that organized calcium oxalate deposits along leaf veins are not unique to the *Ficus* genus but are present in many different leaves (Scott, 1941; Franceschi and Horner, 1980; Doaigey, 1991; Zindler-Frank, 1995; Lersten and Horner, 2000). Therefore, these minerals are thought to fulfill an important, but as yet unknown, function. Note, however, that many leaves do not contain minerals; therefore, the functions of minerals in the leaves that do contain minerals should be regarded as augmenting an existing leaf function or producing a new function for that specific leaf or group of leaves.

This study of 10 different *Ficus* species (two of which are from different geographic areas) shows that there is no correlation between mineralization in the leaf and the environment in which the tree grows, or whether the species is wild or domesticated. In fact, within the same species, mineral contents, together with mineral morphologies and locations, can be highly preserved in plants from different environments. The results indicate that, in the *Ficus* genus, genetic factors are predominant for determining mineral formation compared with environmental parameters such as temperature, water, and light availability. We emphasize that these conclusions are based only on the 10 species and 12 cases studied here.

Four of the *Ficus* species examined contain large elongated cystoliths on the adaxial side. Adaxial cystoliths have been shown to scatter light deep into the mesophyll and, by so doing, enhance photosynthesis (Gal et al., 2012a). Large crystalline calcium oxalate druses can fulfill the same function in okra, *P. obtusifolia*, and pecan (*Carya illinoinensis*) leaves (Gal et al., 2012a; Horner, 2012; Horner et al., 2012; Pierantoni et al., 2017). The scattering properties of the mineral bodies depend on

the refractive index and on the morphology of the scattering object. Both crystalline druses and amorphous cystoliths have geometries that are well suited for light scattering. Furthermore, amorphous materials are isotropic, such that light is scattered uniformly in all directions.

The function of adaxial cystoliths as light scatterers is consistent with the observation that, in these four species, silica deposition never covers the cystoliths. As silica does absorb some light in the visible range, this would reduce the effectiveness of the cystoliths (Pierantoni et al., 2017).

We also noted that these large cystoliths are distributed more or less at regular distances from each other, and this would essentially spread the scattered light evenly throughout the mesophyll. Note that these large cystoliths are never located directly above veins.

The silica in the cell walls on the adaxial side, if present at all, is in the outer epidermal layer, and as silica strongly absorbs UV radiation, it may protect the underlying cells from UV damage. We also observed that, when large cystoliths are present on the adaxial side, the trichomes, if present, are not silicified. This too could be an indication that silicified trichomes may reduce the photon flux to the cystoliths.

When the abaxial side is the principal site for mineral deposition, spherical cystoliths are densely packed and can be found below veins. Furthermore, when the main cystoliths are abaxial, silica is deposited abundantly in the trichomes and in the epidermis cell walls. The silica and cystoliths never spatially overlap. In seven of the *Ficus* species, the abaxial side contains silicified trichomes in the form of prominent thin hairs or shorter spikes. We assume that these trichomes function in leaf defense against herbivores (Hanley et al., 2007; Strömberg et al., 2016). In *F. exasperata* leaves, the ACC silica spikes appear to be particularly complex composite defense units to discourage herbivores.

When abaxial cystoliths are deposited together with adaxial cystoliths, their distribution is more organized, and only rarely are they found below veins. If, instead, cystoliths are deposited only abaxially, their distribution is denser and less organized. One function of adaxial cystoliths in enhancing the photosynthetic efficiency of the leaves already has been established in *F. microcarpa* (Gal et al., 2012a). Micromodulated fluorimetry measurements performed on *F. microcarpa* and *F. carica*, both having abaxial cystoliths, show that these also function as efficient light scatterers from the abaxial side in *F. microcarpa* but not in *F. carica*. One evident difference between the two leaves is in the dense mesophyll layer juxtaposed to the abaxial epidermis, which is present in *F. microcarpa*. Adaxial and abaxial cystoliths cooperate, scattering light that illuminates the central 70 µm of the leaf, which otherwise would not be reached by light. This is apparently not necessarily advantageous in *F. carica*, where the less dense mesophyll can be penetrated by light from the abaxial side through the large air compartments. We do not know what the function of the cystoliths is on the abaxial side in *F. carica*. Unfortunately, the other three species that have abaxial cystoliths only could not be tested because they are not available fresh under fully hydrated conditions. The functions of cystoliths that do not involve light harvesting are yet to be understood. One function might involve the spherical abaxial cystoliths contributing to the mechanical properties of the leaf to maintain shape or orientation. This hypothesis, however, needs to be tested.

CONCLUSION

This study shows that each *Ficus* leaf has an individual system of minerals that seems to be strongly preserved in different environments. Even if each mineral system is unique, there are two main general patterns for mineralization that depend on the preferential side of the leaf for mineral deposition.

ACC cystoliths, calcium oxalates, and silica are not deposited independently, but the mineralization is possibly controlled in unison by the leaf. The silica-oxalates-ACC controlled mutual organization points to the fact that different mineral deposits in leaves should be studied together to better understand the leaf control of mineral deposition and the functions that the minerals fulfill in the leaf.

The functions of cystoliths can vary. Adaxial cystoliths are involved in light redistribution and photosynthesis optimization. Abaxial cystoliths also can be involved in the optimization of light distribution or not, depending on the cellular architecture of the leaf. Other functions that cystoliths may perform, not related to light scattering, have yet to be identified.

MATERIALS AND METHODS

Leaf Samples

Leaves from trees on the Weizmann Institute of Science campus (Rehovot, Israel) were freshly collected and immediately scanned. Leaves from Kibale National Park (southwestern Uganda), Ugalla (Issa Valley, Tanzania), and Bologna (Italy) were collected and immediately immersed in 96% (v/v) pure ethanol.

MicroCT

Cross-Sectional Perspectives of Leaf Anatomy, Cystoliths, and Trichomes

Six leaves were measured from *Ficus microcarpa*, *Ficus elastica*, *Ficus binnendijkij*, and *Ficus carica*, three leaves from *Ficus religiosa*, and one leaf from *Ficus lutea*, *Ficus varifolia*, *Ficus mucoso*, *Ficus sp*, and *Ficus exasperata*. MicroCT scans were acquired using a Micro XCT-400 (Zeiss X-Ray Microscopy). The samples were prepared as described (Pierantoni et al., 2017). Rectangular sections (base, 1 cm; length, 2 cm) were cut from the leaves. The sections were placed in a polypropylene rectangular custom-made container (internal size, 1.7 × 7.7 × 29.7 mm; thickness, 2 mm) that keeps the sample straight and vertical. The container was positioned on the standard microCT stage. In the case of leaves that were preserved in ethanol, the analyzed sections were kept completely immersed in ethanol. In the case of fresh leaves, one of the section extremities was kept in water while the scan was performed above, in air. Tomographic images were obtained by taking 1,300 projections (180°) at 40 kV and 800 µA. The final voxel size was 1.6 µm. 3D volumes were produced using the Avizo 3D analysis software.

Veins and Calcium Oxalates

Triangular sections of leaves (base, 1 cm; length, 2 cm) were cut and placed in a previously sealed plastic pipette tip. To prevent dehydration, the tips were partially filled with water, leaving part of the leaf in air. Only the part of the leaf not immersed in water was imaged.

The scan was performed keeping the source and the detector at the optimal distances for phase-contrast propagation (50 mm and 80–85 mm to the sample, respectively). Phase contrast improves the quality of images by increasing contrast sensitivity, especially around edges (Wilkins et al., 1996). This enabled the detection of minute structures in the soft tissues of the leaf and the accurate identification of mineral structure positions within the soft tissue anatomy. The tomographic images were obtained by taking 1,300 projections (180°) at 30 kV and 450 µA. The final voxel size was 1 µm.

Calculation of the Volume Percentage Occupied by Calcium Minerals in the Leaf

The volume percentage occupied by calcium minerals in the leaf was calculated using the Avizo 3D analysis software. The mineral volume fraction was obtained by selecting the minerals that are the most absorbing bodies in the leaf by contrast thresholding. The leaf total volume was calculated by manual segmentation and interpolation of the selected volume segments. The reproducibility of the values was estimated by repeating the measurements three times in different leaf portions. A variance of 0.2% was obtained.

Light Intensity Measurements

Light intensity was measured at different times of the day using a diode-based power sensor (PD300; Ophir Photonics). The sensor was placed above and below leaves of *F. carica* and *F. microcarpa* trees to measure the exact light intensity reaching the leaf surfaces.

Micromodulated Fluorimetry

To perform leaf autofluorescence measurements, a microfluorimeter setup was custom built around a commercial microscope (Eclipse Ti-U; Nikon) as described (Pierantoni et al., 2017). A 635-nm pulsed diode laser (EPL635; Edinburgh Instruments) emitting pulses with a 100-ps duration at a 20-MHz

repetition rate excited the chlorophyll in the leaf. The beam was focused through a 250-mm focal length lens (LA1461; Thorlabs) onto the back aperture of an objective lens (20×, 0.4 numerical aperture; Nikon). As a result, an ~11-µm-diameter spot was formed in the sample plane. Control over the laser excitation power was achieved by using a variable retarder between two cross-polarized linear polarizers, and a mechanical shutter was used to start and stop illumination periods. Fluorescence light was collected through the same objective, filtered from the direct illumination of the laser by a dichroic mirror (650LP Semrock) and a dielectric filter (635LP Semrock), and imaged onto an electron-multiplying CCD camera (iXon Ultra 897; Andor). The camera captured a 50-s-long frame series with an ~20-ms exposure time to accurately capture the fluorescence dynamics. Dynamic traces started with 5 s without any excitation followed by a dim excitation period (typically 1 nW, matching a flux of $\sim 60 \frac{\mu mol \ \ (ph)}{m^2 s}$) with a 5-s duration in order to obtain the photoluminescence quantum yield for unsaturated reaction centers, followed by a 10-s dark period, followed by another period (30 s) of saturating excitation power (typically 15 nW, matching a flux of $\sim 900 \frac{\mu mol \ \ (ph)}{m^2 s}$). Integrated fluorescence intensities (Fig. 7, A–D) were calculated by summing the electron-multiplying CCD signal over the entire saturating period (30 s) on an ~80-µm^2 region of interest. The data were recorded and analyzed with a custom-written MATLAB script.

In our previous work, we used an extended version of the Munk-Kulbeka model to show that anatomical differences associated with the on-minerals and off-minerals locations cannot be the sole reason for the large fluorescence intensity differences (Pierantoni et al., 2017).

Confocal Microscopy

Sections of *F. microcarpa* veins (about 150 µm thick) were cut along the phloem. The samples were imaged in transmission with a confocal FW1000 laser scanning microscope (Olympus IX81). The volumes were acquired with 20× objective lens magnification, with Z steps of 1.5 µm. Note that at 20× magnification, less than 50 µm of tissue can be imaged.

Supplemental Data

The following supplemental materials are available.

Supplemental Figure S1. MicroCT images of secondary cystoliths deposited in the lower epidermis.

Supplemental Figure S2. MicroCT volume images of *F. elastica* and *F. carica* showing cystoliths and calcium oxalates in reciprocal locations.

Supplemental Figure S3. Calcium oxalate crystal deposition along the central vein in *F. carica* leaves.

Supplemental Figure S4. Confocal image of a phloem section from *F. microcarpa*.

Supplemental Figure S5. Transmitted light wide-field images and logarithmic color scale representation of measured chlorophyll fluorescence intensity for *F. microcarpa* adaxial and abaxial surfaces, *F. carica* adaxial surface, and *F. carica* abaxial surface.

Supplemental Table S1. Light intensity measurements of direct light reaching the leaf adaxial side and of reflected light reaching the leaf abaxial side.

ACKNOWLEDGMENTS

We thank Assaf Gal and Tamir Klein for sharing their knowledge in plant physiology and Neta Varsano for helping with image processing. We thank the Uganda Wildlife Authority and the Uganda National Council for Science and Technology for permission to conduct research in Kibale National Park and the Makerere University Biological Field Station for permission to use the facilities at Ngogo. We also thank the Tanzanian Wildlife Research Institute and the Commission for Science and Technology for permission to conduct research in the Issa Valley, Tanzania. We thank the University of California San

Diego/Salk Center for Academic Research and Training in Anthropogeny for supporting the Ugalla Primate Project and long-term research in the Issa Valley. And we convey our gratitude to the directors and staff at both sites who made the research possible and enjoyable.

FOOTNOTES

[1]This research was partially funded by the Max Planck-Weizmann Center for Integrative Archaeology and Anthropology. L.A. is the recipient of the Dorothy and Patrick Gorman Professorial Chair of Biological Ultrastructure, and S.W. is the recipient of the Dr. Trude Burchardt Professorial Chair of Structural Biology.

REFERENCES

- Ajello L. (1941) Cytology and cellular interrelations of cystolith formation in *Ficus elastica*. Am J Bot 28: 589–594 [Google Scholar]
- Araújo ND, Coelho VPM, Ventrella MC, Agra MdeF. (2014) Leaf anatomy and histochemistry of three species of *Ficus sect. Americanae* supported by light and electron microscopy. Microsc Microanal 20: 296–304 [PubMed] [Google Scholar]
- Arnott H. (1982) Three systems of biomineralization in plants with comments on the associated organic matrix. *In* Biological Mineralization and Demineralization. Springer, Berlin, Heidelberg, pp. 199–218 [Google Scholar]
- Arnott HJ, Pautard FGE. (1970) Calcification in plants. *In* Schraer H, editor. , ed, Biological Calcification: Cellular and Molecular Aspects. Springer, Boston, Springer: pp. 375–446 [Google Scholar]
- Cai K, Gao D, Chen J, Luo S. (2009) Probing the mechanisms of silicon-mediated pathogen resistance. Plant Signal Behav 4: 1–3 [PMC free article] [PubMed] [Google Scholar]
- Chantarasuwan B, Baas P, Van Heuven BJ, Baider C, Van Welzen PC. (2014) Leaf anatomy of *Ficus subsection Urostigma* (*Moraceae*). Bot J Linn Soc 175: 259–281 [Google Scholar]
- Choong MF. (1996) What makes a leaf tough and how this affects the pattern of *Castanopsis fissa* leaf consumption by caterpillars. Funct Ecol 10: 668–674 [Google Scholar]
- Corner E. (1952) Wayside Trees of Malaya, Vol. 1 Government Printing Office, Singapore, pp 147–148 [Google Scholar]
- Currie HA, Perry CC. (2007) Silica in plants: biological, biochemical and chemical studies. Ann Bot 100: 1383–1389 [PMC free article] [PubMed] [Google Scholar]
- De Lucia EH, Shenoi HD, Naidu SL, Day TA. (1991) Photosynthetic symmetry of sun and shade leaves of different orientations. Oecologia 87: 51–57 [PubMed] [Google Scholar]
- Detmann KC, Araújo WL, Martins SC, Sanglard LM, Reis JV, Detmann E, Rodrigues FA, Nunes-Nesi A, Fernie AR, DaMatta FM. (2012) Silicon nutrition increases grain yield, which, in turn, exerts a feed-forward stimulation of photosynthetic rates via enhanced mesophyll conductance and alters primary metabolism in rice. New Phytol 196: 752–762 [PubMed] [Google Scholar]
- Doaigey AR. (1991) Occurrence, type, and location of calcium oxalate crystals in leaves and stems of 16 species of poisonous plants. Am J Bot 78: 1608–1616 [Google Scholar]
- Finley DS. (1999) Patterns of calcium oxalate crystals in young tropical leaves: a possible role as an anti-herbivory defense. Rev Biol Trop 47: 27–31 [Google Scholar]
- Franceschi VR, Horner HT. (1980) Calcium oxalate crystals in plants. Bot Rev 46: 361–427 [Google Scholar]
- Franceschi VR, Nakata PA. (2005) Calcium oxalate in plants: formation and function. Annu Rev Plant Biol 56: 41–71 [PubMed] [Google Scholar]
- Fukushima K, Hasebe M. (2014) Adaxial-abaxial polarity: the developmental basis of leaf shape diversity. Genesis 52: 1–18 [PubMed] [Google Scholar]
- Gal A, Brumfeld V, Weiner S, Addadi L, Oron D. (2012a) Certain biominerals in leaves function as light scatterers. Adv Mater 24: OP77–OP83 [PubMed] [Google Scholar]
- Gal A, Hirsch A, Siegel S, Li C, Aichmayer B, Politi Y, Fratzl P, Weiner S, Addadi L. (2012b) Plant cystoliths: a complex functional biocomposite of four distinct silica and amorphous calcium carbonate phases. Chemistry 18: 10262–10270 [PubMed] [Google Scholar]

- Gal A, Weiner S, Addadi L. (2010) The stabilizing effect of silicate on biogenic and synthetic amorphous calcium carbonate. J Am Chem Soc 132: 13208–13211 [PubMed] [Google Scholar]
- Gautam P, Lal B, Tripathi R, Shahid M, Baig M, Raja R, Maharana S, Nayak A. (2016) Role of silica and nitrogen interaction in submergence tolerance of rice. Environ Exp Bot 125: 98–109 [Google Scholar]
- Hanley ME, Lamont BB, Fairbanks MM, Rafferty CM. (2007) Plant structural traits and their role in anti-herbivore defence. Perspect Plant Ecol Evol Syst 8: 157–178 [Google Scholar]
- Harrison RD. (2005) Figs and the diversity of tropical rainforests. Bioscience 55: 1053–1064 [Google Scholar]
- Herre EA, Jandér KC, Machado CA. (2008) Evolutionary ecology of figs and their associates: recent progress and outstanding puzzles. Annu Rev Ecol Evol Syst 39: 439–458 [Google Scholar]
- Horner HT. (2012) *Peperomia* leaf cell wall interface between the multiple hypodermis and crystal-containing photosynthetic layer displays unusual pit fields. Ann Bot 109: 1307–1316 [PMC free article] [PubMed] [Google Scholar]
- Horner HT, Franceschi VR, Hill EL. (1978) Plant and animal calcium-oxalate crystals. J Cell Biol 79: A38 [Google Scholar]
- Horner HT, Samain MS, Wagner ST, Wanke S. (2015) Towards uncovering evolution of lineage-specific calcium oxalate crystal patterns in *Piperales*. Botany 93: 159–169 [Google Scholar]
- Horner HT, Wanke S, Oelschlägel B, Samain MS. (2017) Peruvian window-leaved *Peperomia* taxa display unique crystal macropatterns in high-altitude environments. Int J Plant Sci 178: 157–167 [Google Scholar]
- Horner HT, Wanke S, Samain MS. (2012) A comparison of leaf crystal macropatterns in the two sister genera *Piper* and *Peperomia* (Piperaceae). Am J Bot 99: 983–997 [PubMed] [Google Scholar]
- Janzen DH. (1979) How to be a fig. Annu Rev Ecol Syst 10: 13–51 [Google Scholar]
- Kausch A, Horner H. (1982) A comparison of calcium oxalate crystals isolated from callus cultures and their explant sources. Scan Electron Microsc 1: 199–211 [Google Scholar]
- Kislev ME, Hartmann A, Bar-Yosef O. (2006) Early domesticated fig in the Jordan Valley. Science 312: 1372–1374 [PubMed] [Google Scholar]
- Kuo-Huang LL, Ku MS, Franceschi VR. (2007) Correlations between calcium oxalate crystals and photosynthetic activities in palisade cells of shadeadapted *Peperomia glabella*. Bot Stud (Taipei, Taiwan) 48: 155–164 [Google Scholar]
- Law C, Exley C. (2011) New insight into silica deposition in horsetail (*Equisetum arvense*). BMC Plant Biol 11: 112. [PMC free article] [PubMed] [Google Scholar]
- Lersten N, Horner H. (2000) Calcium oxalate crystal types and trends in their distribution patterns in leaves of *Prunus* (Rosaceae: Prunoideae). Plant Syst Evol 224: 83–96 [Google Scholar]
- Lucas PW, Choong MF, Tan HTW, Turner IM, Berrick AJ. (1991) The fracture-toughness of the leaf of the dicotyledon *Calophyllum inophyllum* L (Guttiferae). Philos Trans R Soc Lond B Biol Sci 334: 95–106 [Google Scholar]
- Lwanga JS, Butynski TM, Struhsaker TT. (2000) Tree population dynamics in Kibale National Park, Uganda 1975-1998. Afr J Ecol 38: 238–247 [Google Scholar]
- Marschner H, Oberle H, Cakmak I, Römheld V. (1990) Growth enhancement by silicon in cucumber (*Cucumis sativus*) plants depends on imbalance in phosphorus and zinc supply. Plant Soil 124: 211–219 [Google Scholar]
- McNaughton S, Tarrants J, McNaughton M, Davis R. (1985) Silica as a defense against herbivory and a growth promotor in African grasses. Ecology 66: 528–535 [Google Scholar]
- Meyen J. (1839) Materiaux pour servir a l'histoire du developpement des diverses parties dans les plantes. Annales des Sciencies Naturelles Botanique [Google Scholar]
- Omori M, Watabe N. (1980) The Mechanisms of Biomineralization in Animals and Plants. Tokai University Press, Tokyo [Google Scholar]
- Papageorgiou GC. (2007) Chlorophyll a fluorescence: a signature of photosynthesis. Springer Science and Business Media (Vol. 19) [Google Scholar]

- Patiño S, Herre EA, Tyree MT. (1994) Physiological determinants of *Ficus* fruit temperature and implications for survival of pollinator wasp species: comparative physiology through an energy budget approach. Oecologia 100: 13–20 [PubMed] [Google Scholar]
- Perry CC, Fraser MA. (1991) Silica deposition and ultrastructure in the cell-wall of *Equisetum arvense*: the importance of cell-wall structures and flow-control in biosilicification. Philos Trans R Soc Lond B Biol Sci 334: 149–157 [Google Scholar]
- Piel AK, Lenoel A, Johnson C, Stewart FA. (2015) Deterring poaching in western Tanzania: the presence of wildlife researchers. Glob Ecol Conserv 3: 188–199 [Google Scholar]
- Pierantoni M, Tenne R, Brumfeld V, Kiss V, Oron D, Addadi L, Weiner S. (2017) Plants and light manipulation: the integrated mineral system in okra leaves. Adv Sci (Weinh) 4: 1600416. [PMC free article] [PubMed] [Google Scholar]
- Powles SB. (1984) Photoinhibition of photosynthesis induced by visible light. Annu Rev Plant Physiol 35: 15–44 [Google Scholar]
- Scott FM. (1941) Distribution of calcium oxalate crystals in *Ricinus communis* in relation to tissue differentiation and presence of other ergastic substances. Bot Gaz 103: 225–246 [Google Scholar]
- Setoguchi H, Okazaki M, Suga S. (1989) Calcification in higher plants with special reference to cystoliths. *In* Origin, Evolution, and Modern Aspects of Biomineralization in Plants and Animals. Springer, pp. 409–418 [Google Scholar]
- Stewart FA, Piel AK. (2014) Termite fishing by wild chimpanzees: new data from Ugalla, western Tanzania. Primates 55: 35–40 [PubMed] [Google Scholar]
- Strömberg CA, Di Stilio VS, Song Z. (2016) Functions of phytoliths in vascular plants: an evolutionary perspective. Funct Ecol 30: 1286–1297 [Google Scholar]
- Sugimura Y, Mori T, Nitta I, Kontani E, Furosawa T, Tatsumi M, Shin-Ichi K, Wada M, Morita Y. (1999) Calcium deposition in idioblasts of mulberry leaves. Ann Bot (Lond) 83: 543–550 [Google Scholar]
- Tooulakou G, Giannopoulos A, Nikolopoulos D, Bresta P, Dotsika E, Orkoula MG, Kontoyiannis CG, Fasseas C, Liakopoulos G, Klapa MI. (2016) Alarm photosynthesis: calcium oxalate crystals as an internal CO2 source in plants. Plant Physiol 171: 2577–2585 [PMC free article] [PubMed] [Google Scholar]
- Trembath-Reichert E, Wilson JP, McGlynn SE, Fischer WW. (2015) Four hundred million years of silica biomineralization in land plants. Proc Natl Acad Sci USA 112: 5449–5454 [PMC free article] [PubMed] [Google Scholar]
- Watts DP, Potts KB, Lwanga JS, Mitani JC. (2012) Diet of chimpanzees (*Pan troglodytes schweinfurthii*) at Ngogo, Kibale National Park, Uganda. 1. Diet composition and diversity. Am J Primatol 74: 114–129 [PubMed] [Google Scholar]
- Webb MA. (1999) Cell-mediated crystallization of calcium oxalate in plants. Plant Cell 11: 751–761 [PMC free article] [PubMed] [Google Scholar]
- Webb MA, Arnott HJ. (1981) An ultrastructural-study of druse crystals in okra cotyledons. Scan Electron Microsc 285–292 [Google Scholar]
- Wilkins S, Gureyev TE, Gao D, Pogany A, Stevenson A. (1996) Phase-contrast imaging using polychromatic hard x-rays. Nature 384: 335 [Google Scholar]
- Zindler-Frank E. (1995) Calcium, calcium oxalate crystals, and leaf differentiation in the common bean (*Phaseolus vulgaris* L.). Plant Biol 108: 144–148 [Google Scholar]
- Zotz G, Harris G, Königer M, Winter K. (1995) High rates of photosynthesis in the tropical pioneer tree, Ficus insipida Willd. Flora 190: 265–272 [Google Scholar]